International Journal of Heat and Mass Transfer 52 (2009) 2956–2965

Contents lists available at ScienceDirect

International Journal of Heat and Mass Transfer

journal homepage: www.elsevier.com/locate/ijhmt

Numerical simulation of turbulent fluid flow and heat transfer characteristics in heat exchangers fitted with porous media

Yue-Tzu Yang *, Ming-Lu Hwang

Department of Mechanical Engineering, National Cheng Kung University, Tainan 70101, Taiwan

ARTICLE INFO

Article history:
Received 23 August 2008
Received in revised form 19 February 2009
Accepted 19 February 2009
Available online 3 April 2009

Keywords:
Turbulent flow
Porous media
Heat transfer enhancement
Numerical calculation

ABSTRACT

Numerical simulations have been carried out to investigate the turbulent heat transfer enhancement in the pipe filled with porous media. Two-dimensional axisymmetric numerical simulations using the k–ε turbulent model is used to calculate the fluid flow and heat transfer characteristics in a pipe filled with porous media. The parameters studied include the Reynolds number (Re = 5000–15,000), the Darcy number (Da = 10^{-1}–10^{-6}), and the porous radius ratio (e = 0.0–1.0). The numerical results show that the flow field can be adjusted and the thickness of boundary layer can be decreased by the inserted porous medium so that the heat transfer can be enhanced in the pipe. The local distributions of the Nusselt number along the flow direction increase with the increase of the Reynolds number and thickness of the porous layer, but increase with the decreasing Darcy number. For a porous radius ratio less than about 0.6, the effect of the Darcy number on the pressure drop is not that significant. The optimum porous radius ratio is around 0.8 for the range of the parameters investigated, which can be used to enhance heat transfer in heat exchangers.

© 2009 Elsevier Ltd. All rights reserved.

1. Introduction

The heat transfer and transport phenomena in the porous media are important processes in many engineering applications, e.g., heat exchanger, pack-sphere bed, electronic cooling, chemical catalytic reactors, heat pipe technology, etc. The objective of thermal management is to ensure that the temperature of each component in an electronic system remains within specified operating limits [1,2], or to ensure the enhancement of forced convection heat transfer in many engineering applications, such as nuclear cooling, heat exchangers, and solar collectors [3,4]. This kind of technical issue was often encountered by the designers of electronic equipments and thermal energy systems, such as compact heat exchangers, heat pipes, electronic cooling, and solar collectors. The conventional air-handling cooling technology is insufficient in such cases therefore a more effective cooling method is required. Webb [5] reviewed and discussed different techniques used for heat transfer enhancement for single and multiphase flows such as vortex generator and mixers. On the other hand, porous media have large contact surface with fluids, which enhance the heat transfer performance. The porous medium not only changes the condition of flow field which gives a thinner boundary layer, but also its heat conduction coefficient which is generally higher than the fluid under investigation. Hence, the introduction of porous medium into a fluid channel efficiently improves the heat transfer performance of fluid channels. The investigation of Lauriat and Ghafir [6] using porous medium to enhance the rate of heat and mass transfer in energy systems shows that the values of Nusselt number are approximately 50% higher than the values predicted for laminar flows in a channel without porous materials. Moreover, it demonstrates that the convective heat transfer coefficient is higher for systems filled with porous material than the systems without porous material due to the higher thermal conductivity of the porous matrix compared with the lower thermal conductivity of the fluid, especially for gaseous flows. The effect of fluid and thermal transport in a two-dimensional channel which contains a heated block or multiple heated blocks was studied by Young and Vafai [7,8]. Their numerical results indicated that smaller, more widely spaced blocks were associated with better heat transfer performance. Narrow gaps between blocks were found to allow upstream thermal transport. The enhancement of heat transfer performance using porous media with large contact surface with fluids was studied by several researchers, Refs. [9–11]. Recently, many studies have focused on the interfacial problem of the fluid-porous media composite system, e.g., Beavers and Joseph [12]. The interfacial problems between the fluid-porous media are very complex. Vafai and Thiyagaraja [13] considered the interface between porous media and external fluid field, the interface between porous media and a solid boundary. Vafai and Kim [14] derived an exact solution which was studied by Beavers and Joseph [12]. In addition, Vafai and Kim [15] also found that the

* Corresponding author. Tel.: +886 6 2757575x62172; fax: +886 6 2352973.
E-mail address: ytyang@mail.ncku.edu.tw (Y.-T. Yang).

0017-9310/$ - see front matter © 2009 Elsevier Ltd. All rights reserved.
doi:10.1016/j.ijheatmasstransfer.2009.02.024

Nomenclature

C	specific heat
C_e	effective specific heat
C_1, C_2	turbulent constant
Da	Darcy number
D_h	hydraulic diameter
e	ratio of the porous medium radius to the pipe radius
F	inertia coefficient
G	production of turbulence energy
Gr	Grashof number
I	turbulence intensity
K	Permeability
k	thermal conductivity
k_e	effective conductivity of porous material
k	turbulent kinetic energy
L	length of the porous medium
L_i	distance from pipe inlet to porous matrix
L_o	distance from porous matrix to pipe outlet
Nu	local Nusselt number
p	pressure
Pe	Peclet number
Pr	Prandtl number
q_w	heat flux of the heated wall
R	dimensionless radius, r/r_0
Re	Reynolds number based on the radius of pipe, $\rho_f u_{in} r_0/\mu_f$
r	radial coordinate
r_0	outer radius of the cylinder
r_p	porous matrix radius
T	temperature
U	dimensionless velocity in the z- direction, u/u_{in}
u, v	velocity in the z- and r-direction
z	axial coordinate
Z	dimensionless axial coordinate, z/r_0

Greek symbols

ε	dissipation rate of turbulent energy
μ	viscosity of fluid
θ	dimensionless temperature, $\theta = \frac{T-T_{in}}{T_w-T_{in}}$ or $\theta = \frac{T-T_{in}}{(q_w r_0)/k_f}$
ρ	density
μ_ℓ, μ_t, μ_e	laminar, turbulent and effective viscosity
σ_k, σ_ε, σ_T	k–ε turbulence model constant for k, ε and T

Subscripts

e	effective
f	fluid
in	at the channel inlet
m	bulk
p	porous medium
w	wall

enhancement of thermal performance of the porous media mainly depends on the ratio of the effective thermal conductivity of the porous media to fluid thermal conductivity. The heat transfer of a flat plate mounted with porous block array was presented by Huang and Vafai [16]. They found that the porous block array significantly reduced the heat transfer rate on the flat plate. On the contrary, different trends were presented by Hadim [17]. Huang and Vafai [18] considered a forced convection problem in an isothermal parallel-plate channel with porous block using a vorticity stream function formulation. They identified that significant heat transfer augmentation can be achieved through the use of multiple emplaced porous blocks. A numerical study of effects of a random porosity model on heat transfer performance of porous media was demonstrated by Fu et al. [19]. The experimental and numerical study of Pavel and Mohamad [20] on heat transfer enhancement for gas heat exchangers fitted with porous media leads to the conclusion that higher heat transfer rate can be achieved using porous inserts at the expense of a reasonable pressure drop. The studies cited herein provide insights into the transfer of heat by porous metallic materials. The results of these investigations reveal that a porous material can be used as an extremely effective heat sink. The numerical investigation of Yucel and Guven [21] on convection cooling enhancement of heated elements in a parallel-plate channels using porous inserts shows that heat transfer can be enhanced by using high-thermal-conductivity porous inserts and the pressure drop increases rapidly along the channel with an increase of the Reynolds number by the insertion of heated elements and porous matrix. Recently, porous materials are employed to promote heat transfer in a channel, and this has received considerable attention and was the focus of several investigations.

In this section, several studies on heat exchangers, heat pipes, and collectors electronic cooling conducted during recent decades are reviewed. Al-Nimr and Alkam [22] studied unsteady non-Darcian forced convection analysis in an annular tube partially filled with a porous material. Chikh et al. [23] investigated analytical solution of non-Darcian forced convection in an annular duct partially filled with a porous medium. Vafai and Kim [24] theoretically investigated fluid mechanics of interface region between a porous medium and fluid layer. Poulikakos and Kazmierczak [25] studied forced convection in a duct partially filled with a porous material. Their investigation indicated that the porous medium inserting into annular tube enhance effectively rate of heat transfer. Recently, Al-Nimr and Alkam's [26,27] research on the problem of forced convection in composite fluid and porous layers indicated that the unsteadiness in the fluid flow is caused either by a sudden change in the imposed pressure gradient or (and) by a sudden change in the velocity of the channel boundaries. Beavers and Joseph [28] first studied the fluid mechanics at the interface between a fluid layer and a porous medium over a flat plate. Their result indicated that a slip-flow boundary condition with one experimentally determined parameter is inconsistent with the experimentally data, and it seems to depend on material parameters, other than the permeability, and in particular on structural parameters characterizing the nature of the porous surface. Poulikakos and Kazmierczak [25] analyzed forced convection in parallel plat ducts and in circular pipes partially filled with porous materials for constant wall heat flux. The same group extended the work presented to numerical results computed for constant wall temperature but for completely filled ducts [29]. Jang and Chen [30] studied numerically using the Darcy–Brinkman–Forchheimer model for the problem of forced convection in channels partially filled with porous media. Their results indicated that the Nusselt number strongly depends on the open space thickness ratio, and a critical value of the porous layer thickness exists at which the Nusselt reaches a minimum. In addition, it is founded that thermal dispersion effect is only significant for small value of open space thickness ratio. Rudraiah [31] investigated the same problem using the Darcy–Brinkman model. Chikh et al. [32] investigated numerically using the Darcy–Brinkman–Forchheimer to model the problem of forced convection in an annular duct partially filled with a porous medium. Chen and Vafai [33] studied free surface momentum and heat transfer in porous domain using a finite difference

scheme. The limitation of the Darcy–Brinkman–Forchheimer model in porous media and at the interface between the clear fluid and porous region was discussed by Nield [34]. Alkam and Al-Nimr [35] investigated numerically the transient response of circular and annular channels partially filled with porous materials under forced convection conditions. Results of these investigations reveal that porous inserts in an annular duct can increase the heat transfer rate of forced convection. Sung et al. [36] numerically studied forced convection from an isolated heat source in a channel with porous medium. The results illustrated that as the thickness of porous substrate increases or the Darcy number decreases, the fluid flow rate increases. Also, as thermal conductivity ratio increases for a fixed Darcy number, the heat transfer rates are augmented. Zhang et al. [37] numerically investigated the enhancement of heat transfer using porous convection-to-radiation converter for laminar flow in a circular duct. Their report indicated the insertion of a porous core in a circular duct not only increases the convective heat transfer, but also enhances the heat transport by radiation. Alkam et al. [38] studied numerically the enhancement of heat transfer in parallel-plate channels by using porous inserts. They found that heat transfer can be enhanced by using high-thermal-conductivity inserts, decreasing the Darcy number, and increasing the microscopic inertial coefficient. Ould-Amer et al. [39] studied forced convection cooling enhancement by the use of porous materials. The results showed that the insertion of a porous material between the blocks may enhance the heat transfer rate on the vertical side of the blocks. Tzeng [40] experimentally and numerically examined the forced convection heat transfer in a rectangular channel filled with sintered bronze beads and periodically spaced heat blocks. The result indicated that such arrangement can be used to improve the cooling performance of heated blocks, where the blocks are used to simulate heated electronic components, by sintered metallic porous media. Recently, Mohamad [41] numerically investigated the heat transfer enhancement in heat exchangers fitted with porous media. He found that partially filling the conduit with porous medium has two advantages. It enhances the rate of heat transfer, and the pressure drop is much less than that for a conduit fully filled with a porous medium. During these years, some investigations were performed with the local thermal non-equilibrium theory. Angirasa [42] numerically studied forced convective heat transfer in metallic fibrous materials. The numerical results showed that the heat transfer rate increases with the increasing Reynolds number within a range $5000 \leqslant Re \leqslant 25{,}000$, but is insignificant beyond that range. The heat transfer rate also increases with stagnant thermal conductivity, and decreases with the Darcy number. The fiber thickness was found to have significant influence on thermal dispersion. Tzeng [43] experimentally examined spatial thermal regulation of aluminum foam heat sink using a sintered porous conductive pipe. The experimental results indicated that the conductive pipe in an aluminum foam heat sink was very effective in spatial thermal regulation, especially in a mode with lateral arc gaps, which were approximately along the stream-wise axis and beside the conductive pipe. Tzeng et al. [44] experimental studied the forced convection in asymmetrically heated sintered porous channels with or without periodic baffles. Their data indicated that the wall temperatures measured at the baffle attached to the heated wall were slightly lower than those nearby, especially at high Reynolds numbers. Jiang and Ren [45] numerically investigated the forced convection heat transfer in porous media using a thermal non-equilibrium model. Their results showed that the convection heat transfer in porous media can be predicted numerically using the thermal non-equilibrium model with the ideal constant wall heat flux boundary condition. Alazmi and Vafai [46] numerically studied constant wall heat flux boundary conditions in porous media under local thermal non-equilibrium conditions. It is evident that using different boundary conditions may lead to substantially different results.

The macroscopic modeling of turbulent flows passing through porous media concerns many practical applications such as nuclear reactors, heat exchangers or canopy flows. Limited data exists for the case of the turbulent heat transfer and fluid flow characteristics through a porous medium especially using numerical simulations. The main objective of this work is to analyze turbulent heat transfer enhancement that can be achievable and pressure drop due to fully or partially filling a pipe with porous medium. First, the numerical results of laminar flow case were compared to the available data of Mohamad [41] in order to determine the accuracy of the model. The numerical model was then extended to modify the turbulent flow to get a better simulate of a matrix heat exchanger.

2. Mathematical formulation

The schematic diagram of the physical model and the boundary conditions used in this study are shown in Fig. 1. It involves air flowing through a pipe fully or partially filled with porous layer at the core of the conduit for a constant wall temperature and a constant heat flux boundary. The air enters the pipe at a uniform temperature T_{in} and a uniform velocity u_{in}. The thermophysical properties of the fluid and the porous matrix are assumed to be constant, and the porous medium is considered homogeneous (the channel effect near the wall is neglected because the porous medium is sintered bronze beads), isotropic, and non-deformable. In modeling the energy transport, it is assumed that the local equilibrium exists between solid and fluid phases. The thermal equilibrium assumption is valid as far as there is no heat released in the fluid or solid phase. Therefore, the energy equation for the porous medium and the fluid phases based on the local thermal equilibrium is used. Considering the laminar fluid flow due to the resistance of porous medium, the back diffusion can be prevented for low Re values in the energy equation by having longer distance from inlet to porous material. Although a single volume averaged energy equation could have yielded similar results at much lower computational time, the k–ε turbulence model associated with the wall function was used in the numerical calculation for the turbulent flow which highlights the complexity and importance of flow field and temperature field in the vicinity of heated walls. The quantity k/ε provides a natural time scale for the k–ε equations and corresponds physically to a large-scale eddy lifetime, which goes to zero at a wall. This means that the solution can evolve quickly in the near-wall zone and hence should converge rapidly, subsequently responding passively to changes in the rest of the flow. However, the k–ε equations have the potential for generating

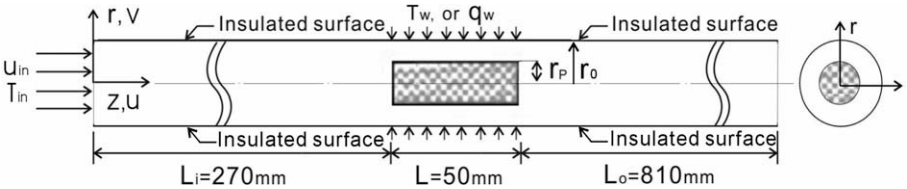

Fig. 1. Schematic diagram of numerical domain with boundary conditions.

rapid changes, a property known as stiffness, which requires considerable care in order to avoid numerical instability. In this study, the non-Darcy model is used to demonstrate the flow behavior inside the porous region. Mathematical formulation of the present problem is based on two-dimensional axisymmetric, steady, turbulent, and incompressible flow with constant properties and negligible buoyancy effects, $Gr/Re^2 \ll 1$. The governing equations to be considered are the time-averaged continuity, momentum, and energy equations. Hence, the governing equations for the fluid region can be written as:

Continuity equation

$$\frac{1}{r}\left[\frac{\partial}{\partial r}(r\rho_f v)+\frac{\partial}{\partial z}(r\rho_f u)\right]=0. \tag{1}$$

z-Momentum equation

$$\frac{1}{r}\frac{\partial}{\partial r}(r\rho_f vu)+\frac{\partial}{\partial z}(\rho_f uu)-\frac{1}{r}\frac{\partial}{\partial r}\left(\mu_e r\frac{\partial u}{\partial r}\right)-\frac{\partial}{\partial z}\left(\mu_e\frac{\partial u}{\partial z}\right) =-\frac{\partial p}{\partial z}+\frac{1}{r}\frac{\partial}{\partial r}\left(r\mu_e\frac{\partial v}{\partial z}\right)+\frac{\partial}{\partial z}\left(\mu_e\frac{\partial u}{\partial z}\right). \tag{2}$$

r-Momentum equation

$$\frac{1}{r}\frac{\partial}{\partial r}(r\rho_f vv)+\frac{\partial}{\partial z}(\rho_f vu)-\frac{1}{r}\frac{\partial}{\partial r}\left(r\mu_e\frac{\partial v}{\partial r}\right)-\frac{\partial}{\partial z}\left(\mu_e\frac{\partial v}{\partial z}\right) =-\frac{\partial p}{\partial r}+\frac{1}{r}\frac{\partial}{\partial r}\left(r\mu_e\frac{\partial v}{\partial r}\right)-2\frac{\mu_e}{r}\left(\frac{v}{r}\right)+\frac{\partial}{\partial z}\left(\mu_e\frac{\partial u}{\partial r}\right). \tag{3}$$

Turbulent kinetic energy equation

$$\frac{1}{r}\left[\frac{\partial}{\partial r}(r\rho_f vk)+\frac{\partial}{\partial z}(r\rho_f uk)\right] -\frac{1}{r}\left[\frac{\partial}{\partial r}\left(r\left(\mu_\ell+\frac{\mu_t}{\sigma_k}\right)\frac{\partial k}{\partial r}\right)+\frac{\partial}{\partial z}\left(r\left(\mu_\ell+\frac{\mu_t}{\sigma_k}\right)\frac{\partial k}{\partial z}\right)\right] =G-\rho_f\varepsilon. \tag{4}$$

Dissipation rate of turbulent kinetic energy

$$\frac{1}{r}\left[\frac{\partial}{\partial r}(r\rho_f v\varepsilon)+\frac{\partial}{\partial z}(r\rho_f u\varepsilon)\right] -\frac{1}{r}\left[\frac{\partial}{\partial r}\left(r\left(\mu_\ell+\frac{\mu_t}{\sigma_\varepsilon}\right)\frac{\partial \varepsilon}{\partial r}\right)+\frac{\partial}{\partial z}\left(r\left(\mu_\ell+\frac{\mu_t}{\sigma_\varepsilon}\right)\frac{\partial \varepsilon}{\partial z}\right)\right] =\frac{\varepsilon}{k}(C_1G-C_2\rho_f\varepsilon), \tag{5}$$

where $G=\mu_t\left\{2\left[\left(\frac{\partial u}{\partial z}\right)^2+\left(\frac{\partial v}{\partial r}\right)^2+\left(\frac{v}{r}\right)^2\right]+\left(\frac{\partial v}{\partial z}+\frac{\partial u}{\partial r}\right)^2\right\}$.

Energy equation

$$\frac{1}{r}\left[\frac{\partial}{\partial r}(r\rho_f vT)+\frac{\partial}{\partial z}(r\rho_f uT)-\frac{\partial}{\partial r}\left(r\frac{\mu_e}{\sigma_T}\frac{\partial T}{\partial r}\right)-\frac{\partial}{\partial z}\left(r\frac{\mu_e}{\sigma_T}\frac{\partial T}{\partial z}\right)\right] =0. \tag{6}$$

And for the porous medium region the governing equations can be written as:

Continuity equation

$$\frac{1}{r}\frac{\partial}{\partial r}(r\rho_f v)+\frac{\partial}{\partial z}(\rho_f u)=0. \tag{7}$$

z-Momentum equation

$$\frac{\partial}{\partial z}(\rho_f uu)+\frac{1}{r}\frac{\partial}{\partial r}(r\rho_f vu)=-\frac{\partial p}{\partial z}+\frac{\partial}{\partial z}\left[\mu_e\frac{\partial u}{\partial z}\right]+\frac{1}{r}\frac{\partial}{\partial r}\left[r\mu_e\frac{\partial u}{\partial r}\right] -\frac{\mu_e}{K}u-\frac{\rho_f F}{\sqrt{K}}|U|u. \tag{8}$$

r-Momentum equation

$$\frac{\partial}{\partial z}(\rho_f vu)+\frac{1}{r}\frac{\partial}{\partial r}(r\rho_f vv)=-\frac{\partial p}{\partial r}+\frac{\partial}{\partial z}\left[\mu_e\frac{\partial v}{\partial z}\right]+\frac{1}{r}\frac{\partial}{\partial r}\left[r\mu_e\frac{\partial v}{\partial r}\right] -\frac{\mu_\ell}{K}v-\frac{\rho_f F}{\sqrt{K}}|U|v-\frac{\mu_\ell v}{r^2}. \tag{9}$$

where $|U|=\sqrt{u^2+v^2}$.

Energy equation

$$\frac{1}{r}\frac{\partial}{\partial r}(r\rho_e c_e vT)+\frac{\partial}{\partial z}(\rho_e c_e uT)=\frac{1}{r}\frac{\partial}{\partial r}\left(rk_e\frac{\partial T}{\partial r}\right)+\frac{\partial}{\partial z}\left(k_e\frac{\partial T}{\partial z}\right), \tag{10}$$

where K is the permeability, F is the inertial coefficient, k_e is the effective conductivity which depends on both the geometry of the porous medium and the conductivity of the solid. Notably, the Tzeng [40] previously published paper indicated that the relevant empirical coefficients in the present numerical model, such as K, F, and k_e, generally do not have universal values. This is because that these empirical coefficients mainly depend on the geometry of the porous medium, the thermal properties of the solid material and fluid, and the flow rate. Additionally, according to the results of Fu and Huang [19], the local Nusselt number distribution of the random porosity model exhibits higher similarity to those of the constant porosity model than those of the variable porosity model. Therefore, a constant porosity value was used in this numerical simulation.

Boundary conditions are specified as follows:

(1) Inlet boundary conditions:

$$u=u_{in},\ \ v=0,\ \ k=k_{in}=Iu_{in}^2,\ \ \varepsilon=\varepsilon_{in}\frac{k_{in}^{3/2}}{\lambda D_h},\ \ T=T_{in},$$

where I is the turbulence intensity, λ is the length scale constant and D_h is the hydraulic diameter.

(2) The adiabatic wall boundary conditions:

The no-slip boundary condition and no-penetration at the wall boundary condition are defined for the numerical model.

$$u=0,\ \ v=0,\ \ \frac{\partial T}{\partial r}=0.$$

(3) Both the constant wall temperature and constant heat flux boundary conditions are applied on the surface of the heated wall.

$u=0$, $v=0$, $T=T_w$ for the constant wall temperature boundary condition,

$u=0$, $v=0$, $-k\frac{\partial T}{\partial r}=q_w$ for the constant heat flux boundary condition.

(4) Interfacial boundary conditions:

At the porous/fluid interface, the following quantities evaluated in both the porous and fluid regions are matched.

$$u_f=u_p,\ \ v_f=v_p,\ \ p_f=p_p,$$
$$\frac{\partial u_f}{\partial z}=\frac{\partial u_p}{\partial z},\ \ \frac{\partial v_f}{\partial z}=\frac{\partial v_p}{\partial z},$$

$T_f=T_p$, $k_f\frac{\partial T_f}{\partial z}=k_s^*\frac{\partial T_p}{\partial z}$, where k_s^* is the effective conductivity of the solid and depends on both the geometry of the porous medium and the conductivity of the solid, which was given by Tzeng [40].

And $k=\varepsilon=0$

The above conditions express the non-slip condition, the continuity of velocities, pressure, stresses, temperature, and the heat flux.

(5) Exit boundary conditions:

$$P = P_{atm}, \quad \frac{\partial k}{\partial z} = \frac{\partial \varepsilon}{\partial z} = \frac{\partial T}{\partial z} = 0.$$

The outlet boundary is located far enough downstream for conditions to be fully developed.

3. Calculation and validations

In this study, the computational domain was chosen to be larger than the physical domain to eliminate the entrance and exit effect and to satisfy the continuity condition at the exit. The numerical computations were carried out by solving the governing conservation equations with the boundary conditions. A non-uniform grid system with a large concentration of nodes in regions of steep gradients was employed. The numerical method used in the present study is based on the SIMPLE algorithm of Patankar [47]. This is an iterative solution procedure where the computation is begun by guessing the pressure field. The momentum equation is solved to determine the velocity components. Even though the continuity equation does not contain any pressure, it can be transformed easily into a pressure correction equation. The conservation equations are discretized by a control volume based finite difference method with a power-law scheme. The set of difference equations are solved iteratively using a line by line solution method in conjunction with a tridiagonal matrix form. The solution is considered to be converged when the normalized residual of the algebraic equation is less than a prescribed value of 10^{-4}.

The local Nusselt number (Nu) of a constant wall temperature and a constant heat flux on the pipe wall were defined as:

$$Nu = \frac{2\left(\frac{\partial\theta}{\partial R}\right)|_w}{\theta_w - \theta_m}, \quad \text{where } \theta = \frac{T - T_{in}}{T_w - T_{in}}, \theta_m = \frac{\int_0^1 U\theta R dR}{\int_0^1 U R dR}$$

for the constant wall temperature boundary condition, (11)

$$Nu = \frac{q_w r_0}{k_f(T_w - T_{in})} = \frac{1}{\theta_w - \theta_m}, \theta = \frac{T - T_{in}}{(q_w r_0)/k_f}$$

for the constant heat flux boundary condition, (12)

where q_w is the heat flux of the heated wall, the typical case with sample $L = 50$ mm, $L_i = 270$ mm, $L_0 = 810$ mm, $r_0 = 13.5$ mm, $Re = 10^4$, $e = 0.1$, $Da = 10^{-6}$ was used for grid test. A comparison of laminar numerical predictions with the available data in the literature was used to assess the grid independence of the results as shown in Fig. 2a. Different size meshes, 10×160, 15×170, 20×160 and 24×175 in r- and z-directions, respectively, were employed in testing the numerical model. It has been validated for laminar flow using numerical data reported in Mohamad [41], and a good agreement has been found. In this study, the grid independent test for the turbulent flow is also presented in Fig. 2b. Based on the grid independent tests of the velocity profiles as shown in Fig. 2a and b, the mesh size of 20×160 were used for all computations. In addition, the predicated Nusselt number results from grid independent simulations indicate that Nu = 23.28, 25.85, 27.15 and 27.16 for the grid 10×160, 15×170, 20×160 and 24×175. The middle mesh size of 20×160 was used because the Nusselt number differences were less than 0.04%. Therefore, it supports the grid independent test by using the velocity profiles.

4. Results and discussion

The numerical algorithm and computer program were carefully evaluated by comparing model prediction with available laminar pipe flow fully or partially filled with porous medium. After the validation of the numerical calculations, steady turbulent flow in a pipe fully or partially filled with porous medium was considered numerically for a constant wall temperature and a constant heat flux boundary conditions. The relevant parameters were different values of the Reynolds number (Re = 5000–15,000), the Darcy number ($Da = 10^{-1}$–10^{-6}) and the porous radius ratio ($e = 0.0$–1.0).

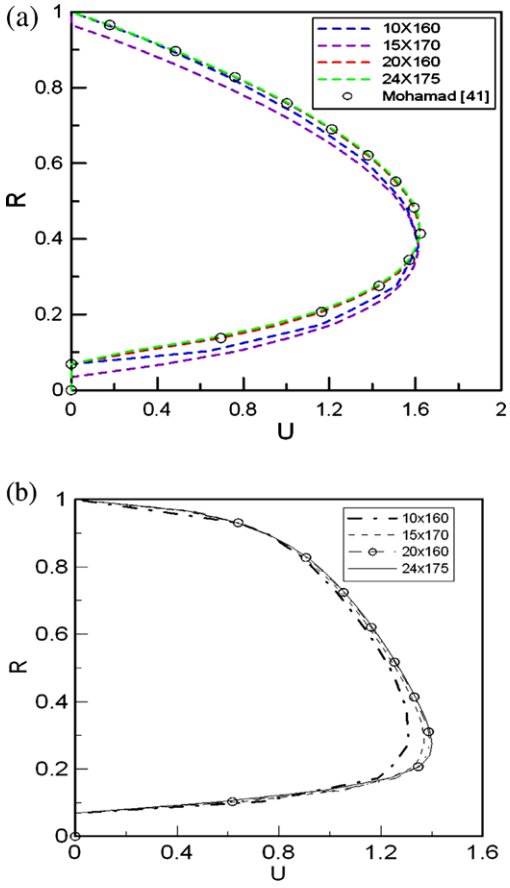

Fig. 2. Grid independent test of velocity profiles for $e = 0.1$, and $Da = 10^{-6}$. (a) $Re = 10^2$, (b) $Re = 10^4$.

In order to validate the numerical code, the typical case was calculated with $e = 0.0$–1.0, $Da = 10^{-6}$, and $Re = 100$, the numerical results of fully developed velocity profiles for different porous radius ratio and the local Nusselt number distribution along the flow direction were compared with the relevant cases reported by Mohamad [41]. Mohamad [41] studied the problem of laminar heat transfer enhancement for a flow in a pipe fully or partially filled with porous inserted at the core of the conduit. Figs. 3 and 4 show the comparison of numerical predictions of velocity profiles and the local Nusselt number distribution between present results and Mohamad's [41] numerical results for $Re = 100$, $Da = 10^{-6}$. In Fig. 3a and b, the velocity profile of fluid flow through porous medium was similar to plug flow. This was due to channeling effects of the porous medium, and the constant porosity of the porous medium. The no-slip boundary condition at the wall caused the steep velocity gradient. For $e = 1.0$, the pipe is completely filled with porous medium and the plug flow assumption is valid. The numerical results agreed well with Mohamad's data [41]. Fig. 3b shows the velocity profile of the laminar flow for different porous radius ratio and the different Zs ($Z = z/r_0 = 25.9$, 81.48). It revealed that the flow is intended to fully developed at $Z = 25.9$, and then the flow arrived to fully developed at $Z = 81.48$. As for the flow in a pipe with porous medium, the local Nusselt number variation along the pipe for different porous radius ratio is shown in Fig. 4.

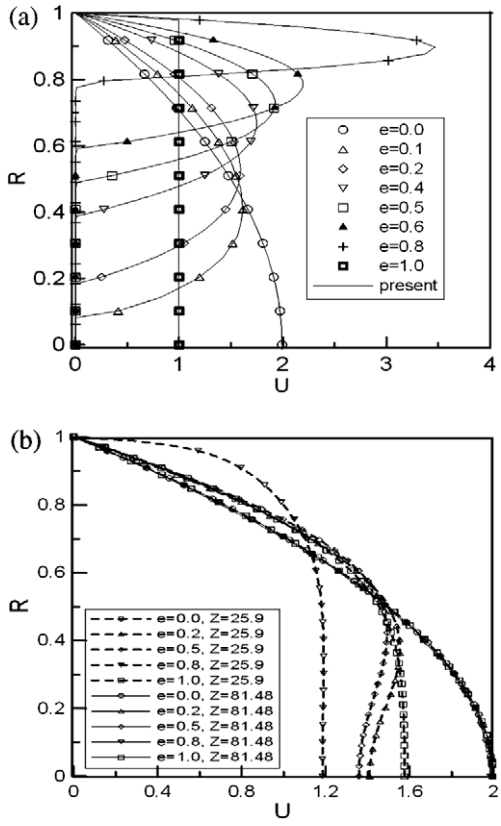

Fig. 3. (a) Comparison of numerical predictions of velocity profiles between present results and Mohamad's [41] numerical results at $Z = 21.85$, (b) the fully developed velocity profiles for Re = 100, Da = 10^{-6}.

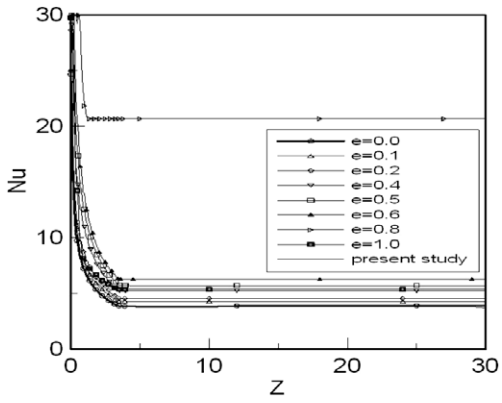

Fig. 4. Comparison of numerical predictions of local Nusselt number distribution along the flow direction between present results and Mohamad's [41] numerical results for Re = 100, Da = 10^{-6}.

It demonstrates that the local Nusselt number increases as the porous radius ratio increases. This is due to the fact that the fluid escapes from the high resistance region (porous medium region) to the outer region. Fig. 5a and b presents the numerical predictions of velocity profiles for different porous radius ratio with Re = 10^4, Da = 10^{-6}. The findings indicated that the turbulent mixing results in a more rapid transfer of momentum between different layers of fluid. Thus, the velocity distribution in a turbulent flow is more uniform than that in a laminar flow, as shown in Fig. 3. This result supports the reports of many investigators. Additionally, the quantity of air that entered the porous medium was lower than the average flow rate, and the flow velocity in the zone of cleared channel was higher than the average velocity. This is due to the fact that the fluid escapes from the high resistance region (porous region) to the outer region. Moreover, it demonstrated that the fluid mainly flows between the porous medium and pipe wall, hence the fluid flowing through the porous medium is negligible. Since the fluid flows between the porous matrix and pipe, the local Nusselt number should be equal to the local Nusselt number for annular flow which will be shown in Fig. 8 subsequently. Fig. 5b shows the velocity profile of turbulent flow for the different porous radius ratio and the different Zs ($Z = z/r_0 = 59.25, 81.48$). It revealed that the flow is intended to fully developed at $Z = 59.25$, and then the flow achieved fully developed at $Z = 81.48$. According to the results of Figs. 3b and 5b, the fully development is validated in laminar or turbulent. The numerical predictions of velocity profiles for different Darcy number at $e = 0.5$, Re = 10^4 is presented in Fig. 6. The numerical results reveal that the flow rate in the porous medium increased as the Darcy number increased, and therefore the plug flow assumption is not valid when Da $\geqslant 10^{-3}$. The comparison results indicate that most of the numerical predications are consistent with the results of investigation by Mohamad [41]. Fig. 7a and b shows the numerical predictions of temperature contours along the flow direction for Re = 10^4, Da = 10^{-6} with a constant wall temperature and a constant heat flux boundary conditions, respectively. It can be seen from the temperature contours of either isothermal or iso-heat flux condition that the temperature changes significantly in the vicinity of heated walls. The insertion of porous medium not only increases flow velocity which enhances the effect of forced convection but also generates turbulence which achieves a thinner boundary layer on heated walls. Both contribute to the enhancement of heat transfer in this region. On the contrary, the temperature variation inside porous medium is not obvious since the fluid velocity is low inside porous medium. This suggests again

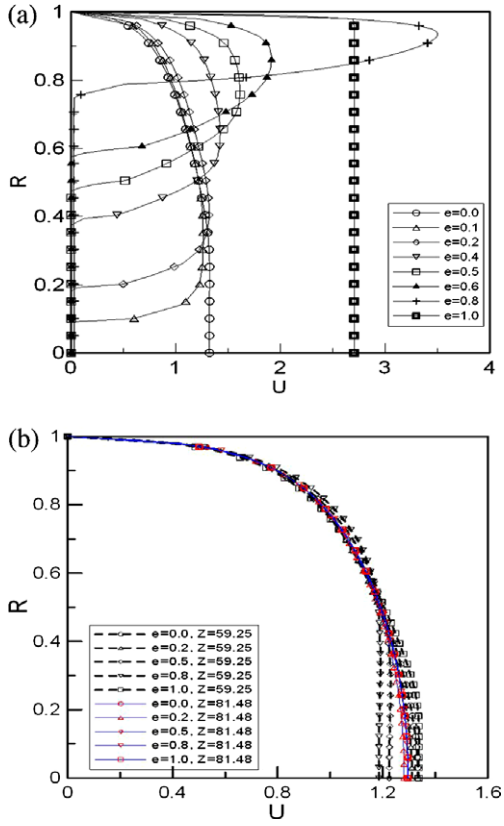

Fig. 5. (a) Numerical predictions of velocity profiles at $Z = 21.85$, (b) the fully developed velocity profiles for different porous radius ratio (Re = 10^4, Da = 10^{-6}).

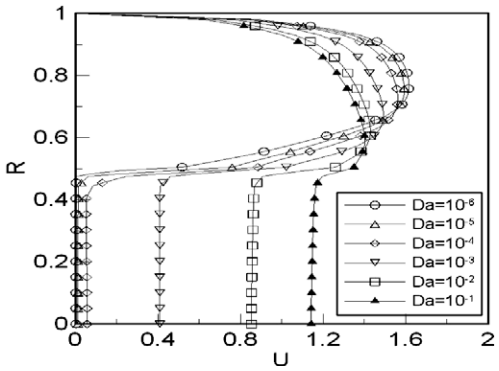

Fig. 6. Numerical predictions of velocity profiles for different Darcy number ($e = 0.5$, $\mathrm{Re} = 10^4$).

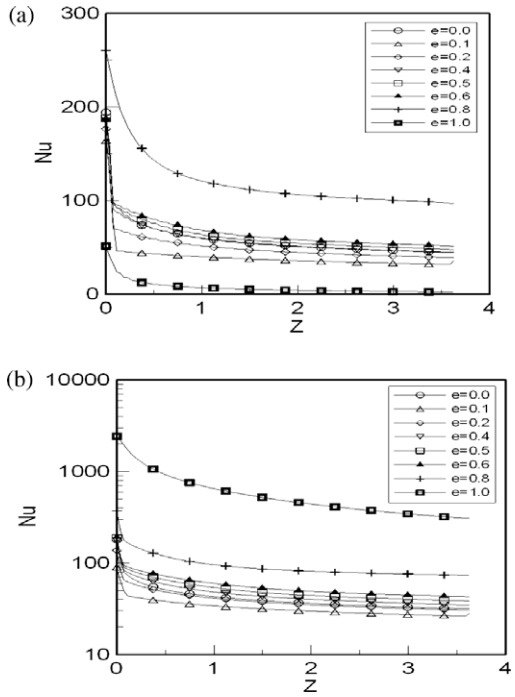

Fig. 8. Numerical predictions of local Nusselt number distribution along the flow direction for $\mathrm{Re} = 10^4$, $\mathrm{Da} = 10^{-6}$. (a) $T_w = 80$ °C, (b) $q_w = 80$ kW/m^2.

that it is reasonable to have a locally quasi-equilibrium model to simulate the flow field inside the porous medium. Fig. 8a and b shows the numerical predictions of the local Nusselt number distribution along the flow direction for $\mathrm{Re} = 10^4$, $\mathrm{Da} = 10^{-6}$ with a constant wall temperature and a constant heat flux boundary condition, respectively. The assumption of a constant wall temperature can be justified as the heat coefficient on the outer surface and the temperature is higher than that on the inner surface which is common in many industrial heat exchanger applications. Fig. 8a indicates that accordingly the boundary layer thickness decreases, the Nusselt number increased as the porous radius increased due to the fact that the fluid escapes from the high resistance region to the outer region. The fluid flows mostly between the porous layer and the pipe wall. Such a channeling effect takes place for $e \leqslant 0.8$. Further increase of the diameter of porous medium decreases the clear gap and fluid experiences high resistance, where the fluid does not have a preferential region to flow, and therefore, the local Nusselt number decreases. Moreover, fully filling the pipe with porous medium will result in the decrease of temperature gradients for the constant wall temperature condition. The heat transfer characteristic of high conductivity of the porous medium can not be obvious. Numerical results reveal that the optimal value is about $e = 0.8$. Fig. 8b demonstrates that the characteristic of heat transfer is consistent except $e = 1.0$ for the isoflux condition compared with the constant wall temperature condition. Although the quantity of air that flows into porous medium was lower but the porous medium with high-thermal-conductivity for the sintered bronze beads ($K = 2.83 \times 10^{-10}$, $F = 0.239$, $k_s = 10.73$) can significantly enhance the effect of heat transfer, the calculations agree with the results of earlier work [21]. According to Yucel and Guven [21] who studied forced convection cooling enhancement of heated elements in a parallel-plate channels using porous inserts, their results revealed that heat transfer can be enhanced by using high-thermal-conductivity porous inserts. On the other hand, the turbulent flow with strong forced convectional effect in channels without porous medium can dissipate the heat from the heating wall. Fig. 8 illustrated the forced convection will decrease as $e < 0.5$. However, the superiority of heat transfer enhancement can be accentuated as $e \geqslant 0.5$.

Next, the turbulent convection heat transfer in a pipe with a constant wall heat flux boundary condition differs from that with a constant wall temperature boundary condition as shown in Figs.

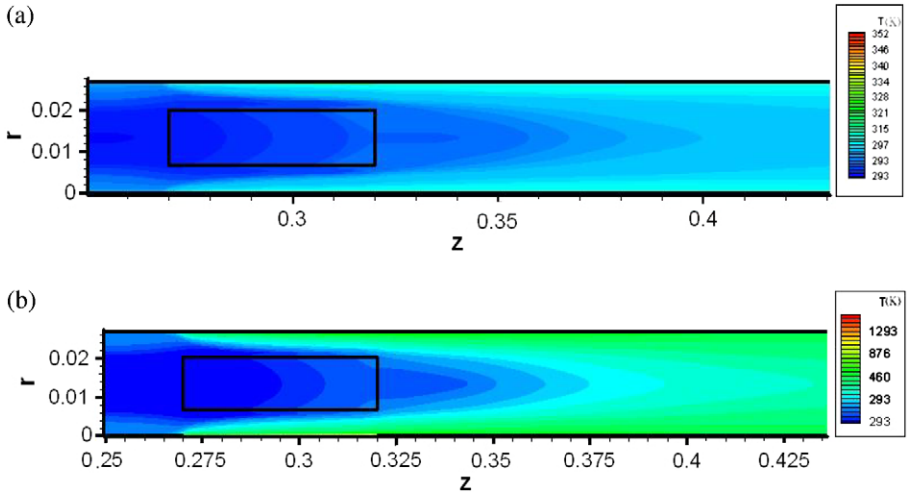

Fig. 7. Numerical predictions of temperature contours along the flow direction for $\mathrm{Re} = 10^4$, $e = 0.5$, $\mathrm{Da} = 10^{-6}$. (a) $T_w = 80$ °C, (b) $q_w = 80$ kW/m^2.

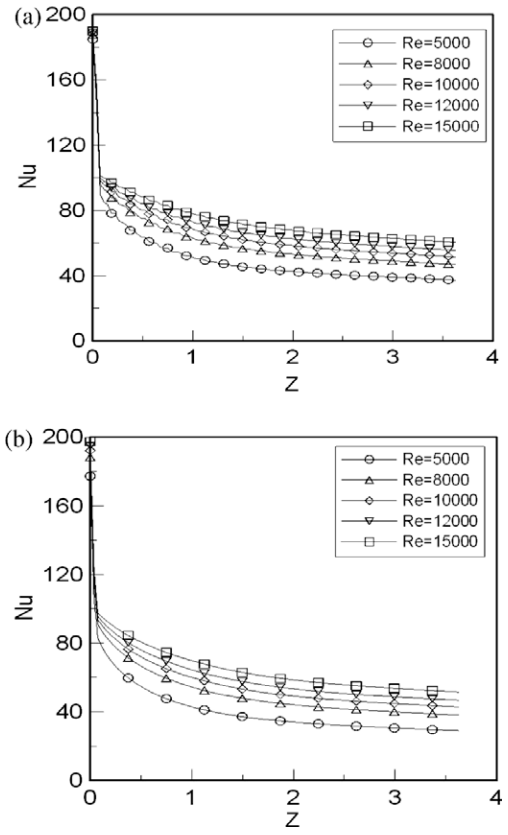

Fig. 9. Numerical predictions of local Nusselt number distribution along the flow direction for different Reynolds number, $e = 0.6$, $Da = 10^{-6}$. (a) $T_w = 80\ ^\circ C$, (b) $q_w = 80\ kW/m^2$.

9 and 10. Fig. 9a and b shows that numerical predictions of the local Nusselt number distribution along the flow direction for different Reynolds number, $e = 0.6$, $Da = 10^{-6}$, and (a) $T_w = 80\ ^\circ C$, (b) $q_w = 80\ kW/m^2$, respectively. Numerical results demonstrated that the local Nusselt number became stronger as Re number increased with the isoflux condition or the constant temperature condition. Fig. 10a and b demonstrates the local Nusselt number as a function of porous radius radio and for a range of Darcy number at $Re = 10^4$, with (a) $T_w = 80\ ^\circ C$, (b) $q_w = 80\ kW/m^2$ boundary conditions, respectively. Fig. 10a shows that heat transfer enhancements increased with increased porous radius ratio and decreased with Darcy number when $e \leqslant 0.8$. The optimum thickness of filled porous medium is about 0.8. Fig. 10b shows the local Nusselt number became larger with increased porous radius ratio, while the effects of the Darcy number is not very obvious at a constant heat flux condition. This result corresponding to Fig. 8b shows that the porous medium with high-thermal-conductivity can significantly enhance the effect of heat transfer. An important factor to be considered in the employment of porous media for the purpose of heat transfer enhancement is the increase of pressure drop. Heat exchanger analyses cannot be completed without pressure drop analysis. Fig. 11a and b presents the numerical predictions of pressure gradients as a function of porous radius ratio and the Darcy number at $Re = 10^4$, with (a) $T_w = 80\ ^\circ C$, (b) $q_w = 80\ kW/m^2$. Fig. 11a and b indicates that for the porous radius ratio which is roughly less than 0.6, the effect of the Darcy number on the pressure drop is not that significant; and the pressure drop increased with the increasing of porous radius ratio especially the pressure drop increased rapidly when porous medium is fully filled in a pipe. The above results suggest partially filling the conduit with porous medium can enhance the rate of heat transfer and the pressure drop can be much less than that for a conduit fully filled with a porous medium. So the porous medium should be partially filled

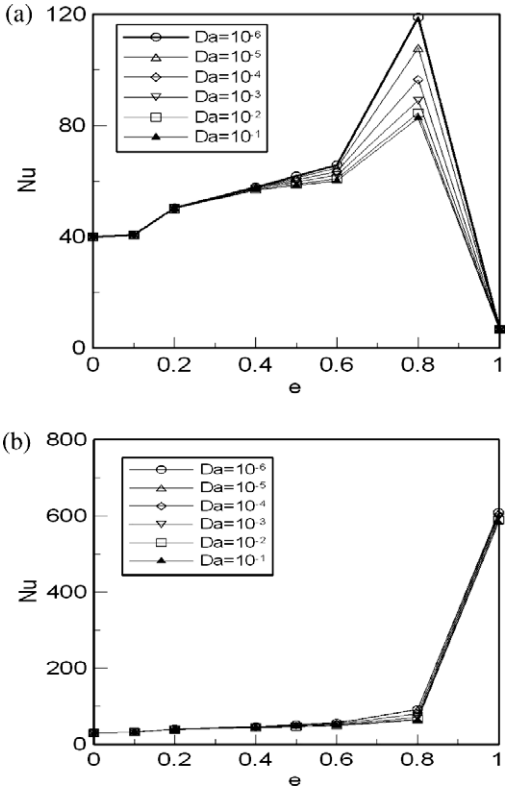

Fig. 10. Numerical predictions of local Nusselt number for different porous ratio, $Re = 10^4$. (a) $T_w = 80\ ^\circ C$, (b) $q_w = 80\ kW/m^2$.

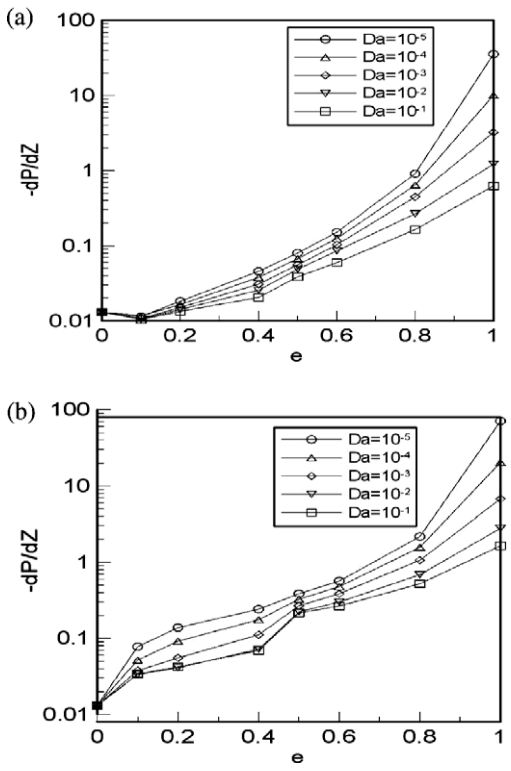

Fig. 11. Numerical predictions of pressure gradients for a pipe flow as a function of porous radius ratio and Darcy number, $Re = 10^4$. (a) $T_w = 80\ ^\circ C$, (b) $q_w = 80\ kW/m^2$.

in the practical application. This study reveals that the optimum thickness of filled porous medium is about $0.6 \leqslant e < 0.8$ for a constant wall temperature condition. Similarly, the optimum thickness of filled porous medium is about $0.6 \leqslant e < 1.0$ for a constant heat flux condition.

5. Conclusions

The present work numerically investigated the fluid flow behavior and heat transfer enhancements in a pipe fully or partially filled with porous medium inserted at the core of the conduit. The relevant parameters were different values of the Reynolds number (Re = 5000–15,000), the Darcy number ($Da = 10^{-1}$–10^{-6}), and the porous radius ratio (e = 0.0–1.0). Conclusions can be summarized as follows:

1. Porous media has large contact surface with fluids which enhance the heat transfer performance. The porous medium not only changes the condition of flow field which gives a thinner boundary layer, but also its heat conduction coefficient which is generally higher than the fluid under investigation. Hence, introducing a porous medium into a fluid channel efficiently improves the heat transfer performance of fluid channels. In this study, although only a small quantity of fluid flows through porous medium, the higher heat conductivity of porous material helps to dissipate the heat generated from wall of a pipe.
2. The turbulent mixing results in a more rapid transfer of momentum between different layers of fluid. Thus, the velocity distribution in a turbulent flow is more uniform than that in a laminar flow. The flow rate in the porous medium increased as the Darcy number increased. Therefore, the plug flow assumption is not valid for $Da \geqslant 10^{-3}$.Additionally, the quantity of air that entered the porous medium was lower than the average flow rate, and the flow velocity in the zone of cleared channel was higher than the average velocity. This is due to the fact that the fluid escapes from the high resistance region (porous region) to the outer region. The above findings demonstrated that the heat transfer efficiency of the turbulent flow is better compared with the laminar flow.
3. The numerical results reveal that heat transfer can be enhanced by using high-thermal-conductivity porous inserts. Moreover, the turbulent flow in the conduit without porous medium can dissipate the heat from the heating wall due to the strong forced convectional effect. The results illustrated that the forced convection will be diluted for $e < 0.5$. However, the superiority of heat transfer enhancement becomes apparent for $e \geqslant 0.5$.
4. Although the rate of heat transfer can be significantly increased by inserting porous medium into the core of a conduit, the rapid increase of pressure drop becomes the major limitation of such application. Partially filling the conduit with porous medium is better than the fully filled one when both the heat transfer rate and pressure drop are considered. The optimum ratio of filled porous radius ratio is about 0.8 according to our simulation and analyses. Under such conditions, the heat transfer can be enhanced significantly while the pressure gradients can be controlled in an acceptable range.

References

[1] J.G. Maveety, H.H. Jung, Design of an optimal pin-fin heat sink with air impingement, Int. Commun. Heat Mass Transfer 27 (2000) 229–240.
[2] G. Hetsroni, A. Mosyak, Z. Segal, G. Ziskind, A uniform temperature heat sink for cooling of electronic devices, Int. J. Heat Mass Transfer 45 (2002) 3275–3286.
[3] M.K. Alkam, M.A. Al-Nimr, Solar collectors with tubes partially filled with porous substrate, ASNE J. Solar Energy Eng. 121 (1999) 20–24.
[4] R. Echigo, H. Yoshida, T. Mochizuki, Temperature equalization by radiative converter for a-slab in continuous casting-direct rolling, in: Proceedings of the Second ASME/JSME Thermal Engineering Joint Conference, vol. 5, 1987, pp. 63–69.
[5] R.L. Webb, Principles of Enhanced Heat Transfer, Wiley, New York, 1994.
[6] G. Lauriat, R. Ghafir, Forced convective transfer in porous media, in: K. Vafai, H.A. Hadim (Eds.), Handbook of Porous Media, Marcel Dekker, New York, 2000, pp. 201–267.
[7] T.J. Young, K. Vafai, Convective cooling of a heated obstacle in a channel, Int. J. Heat Mass Transfer 41 (1998) 3131–3148.
[8] T.J. Young, K. Vafai, Convective flow and heat transfer in a channel containing multiple heated obstacles, Int. J. Heat Mass Transfer 41 (1998) 3279–3298.
[9] K. Vafai, C.L. Tien, Boundary and inertia effects on flow and heat transfer in porous media, Int. J. Heat Mass Transfer 24 (1981) 195–203.
[10] M. Kaviany, Laminar flow through a porous channel bounded by isothermal parallel plates, Int. J. Heat Mass Transfer 28 (1985) 851–858.
[11] R.F. Benenati, C.B. Brosilow, Void fraction distribution in a bed of spheres, AIChE J. 8 (1962) 359–361.
[12] G.S. Beavers, D.D. Joseph, Boundary condition at a naturally permeable wall, J. Fluid Mech. 30 (1967) 197–207.
[13] K. Vafai, R. Thiyagaraja, Analysis of flow and heat transfer at the interface region of a porous medium, Int. J. Heat Mass Transfer 30 (1987) 1391–1405.
[14] K. Vafai, S.J. Kim, Fluid mechanics of the interface region between a porous medium and a fluid layer – an exact solution, Int. J. Heat Fluid Flow 11 (1990) 254–256.
[15] K. Vafai, S.J. Kim, Analysis of surface enhancement by a porous substrate, Trans. ASME. J. Heat Transfer 112 (1990) 700–706.
[16] P.C. Huang, K. Vafai, Flow and heat transfer control over an external surface using a porous block array arrangement, Int. J. Heat Mass Transfer 36 (1993) 4019–4032.
[17] A. Hadim, Forced convection in a porous channel with localized heat source, Trans. ASME J. Heat Transfer 116 (1994) 465–472.
[18] P.C. Huang, K. Vafai, Analysis of forced convection enhancement in a channel using porous blacks, AIAA J. Thermophys. Heat Transfer 8 (1994) 563–573.
[19] W.S. Fu, H.C. Huang, Effects of a random porosity model on heat transfer performance of porous media, Int. J. Heat Mass Transfer 42 (1999) 13–25.
[20] B.I. Pavel, A.A. Mohamad, An experimental and numerical study on heat transfer enhancement for gas heat exchangers fitted with porous media, Int. J. Heat Mass Transfer 47 (2004) 4939–4952.
[21] N. Yucel, R.T. Guven, Forced-convection cooling enhancement of heated elements in a parallel-plate channels using porous inserts, Numer. Heat Transfer Part A 51 (2007) 293–312.
[22] M.A. Al-Nimr, M.K. Alkam, Unsteady non-Darcian forced convection analysis in annuls partially filled with a porous material, ASME J. Heat Transfer 119 (1997) 1–6.
[23] S. Chikh, A. Boumedien, K. Bouhadef, G. Lauriat, Analytical solution of non-Darcian forced convection in an annular duct partially filled with a porous medium, Int. J. Heat Mass Transfer 38 (1995) 1543–1551.
[24] K. Vafai, S.J. Kim, Fluid mechanics of interface region between a porous medium and fluid layer – an exact solution, Int. J. Heat Mass Transfer 11 (1990) 254–256.
[25] D. Poulikakos, M. Kazmierczak, Forced convection in a duct partially filled with a porous material, ASME J. Heat Transfer 109 (1987) 653–662.
[26] M.A. Al-Nimr, M.K. Alkam, Unsteady non-Darcian fluid flow in parallel channels partially filled with porous materials, Heat Mass Transfer 33 (1998) 315–318.
[27] M.K. Alkam, M.A. Al-Nimr, Z.N. Mousa, Transient forced convection of non-Newtonian fluid in the entrance region of porous concentric annuli, Int. Numer. Meth. Heat Fluid Flow 8 (5) (1998) 703–716.
[28] G.S. Beavers, D.D. Joseph, Boundary conditions at naturally permeable wall, J. Fluid Mech. 13 (1967) 197–207.
[29] D. Poulikakos, K. Rwnken, Forced convection in a channel filled with a porous medium, including the effect of flow inertia, variable porosity, and Brinkman friction, ASME J. Heat Transfer 109 (1987) 880–888.
[30] J.Y. Jang, J.L. Chen, Forced convection in a parallel plate channel partially filled with a high porosity medium, Int. Commun. Heat Mass Transfer 19 (1992) 263–273.
[31] N. Rudraiah, Forced convection in a parallel plate channel partially filled with a porous material, ASME J. Heat Transfer 107 (1985) 331–332.
[32] S. Chikh, A. Boumedien, K. Bouhadef, G. Lauriat, Non-Darcian forced convection analysis in an annular partially filled with a porous material, Numer. Heat Transfer A 28 (1995) 707–772.
[33] S.C. Chen, K. Vafai, Analysis of free surface momentum and energy transport in porous media, Numer. Heat Transfer A 29 (1996) 281–296.
[34] D.A. Nield, The limitation of the Brinkman–Forchheimer equation in modeling flow in a saturated porous medium and at an interface, Int. J. Heat Mass Transfer 12 (1991) 269–272.
[35] M.K. Alkam, M.A. Al-Nimr, Transient non-Darcian forced convection flow in a pipe partially filled with a porous material, Int. J. Heat Mass Transfer 41 (1998) 347–356.
[36] H.J. Sung, S.Y. Kim, J.M. Hyun, Forced convection from an isolated heat source in a channel with porous medium, Int. J. Heat Fluid Flow 16 (1995) 527–535.
[37] J.M. Zhang, W.H. Sutton, F.C. Lai, Enhancement of heat transfer using porous convection-to-radiation converter for laminar flow in a circular duct, Int. J. Heat Mass Transfer 40 (1996) 39–48.

[38] M.K. Alkam, M.A. Al-Nimr, M.O. Hamdan, Enhancing heat transfer in parallel-plate channels by using porous inserts, Int. J. Heat Mass Transfer 44 (2001) 931–938.
[39] Y. Ould-Amer, S. Chikh, K. Bouhadef, G. Lauriat, Forced convection cooling enhancement by use of porous materials, Int. J. Heat Fluid Flow 19 (1998) 251–258.
[40] S.C. Tzeng, Convective heat transfer in a rectangular channel filled with sintered bronze bead and periodically spaced heated blocks, Trans. ASME J. Heat Transfer 128 (2006) 453–464.
[41] A.A. Mohamad, Heat transfer enhancements in heat exchangers fitted with porous media. Part I: Constant wall temperature, Int. J. Thermal Sci. 42 (2003) 385–395.
[42] D. Angirasa, Forced convective heat transfer in transfer in metallic fibrous materials, ASME J. Heat Transfer 124 (2002) 739–745.
[43] S.C. Tzeng, Spatial thermal regulation of aluminum foam heat sink using a sintered porous conductive pipe, Int. J. Heat Mass Transfer 50 (1–2) (2007) 117–126.
[44] S.C. Tzeng, T.M. Jeng, Y.C. Wang, Experimental study of forced convection in asymmetrically heated sintered porous channels with/without periodically baffles, Int. J. Heat Mass Transfer 49 (1–2) (2006) 78–88.
[45] P.X. Jiang, Z.P. Ren, Numerical investigation of forced convection heat transfer in porous media using a thermal non-equilibrium model, Int. J. Heat Fluid Flow 22 (1) (2001) 102–110.
[46] B. Alazmi, K. Vafai, Constant wall heat flux boundary conditions in porous media under local thermal non-equilibrium conditions, Int. J. Heat Mass Transfer 45 (2002) 3071–3087.
[47] S.V. Patankar, Numerical Heat Transfer and Fluid Flow, McGraw-Hill, Hemisphere, New York, 1980.